Volume 98, Number 6, November–December 1993
Journal of Research of the National Institute of Standards and Technology

[J. Res. Natl. Inst. Stand. Technol. 98, 679 (1993)]

Pressure-Volume-Temperature Relations in Liquid and Solid Tritium

Volume 98 Number 6 November–December 1993

E. R. Grilly

Los Alamos National Laboratory,
Los Alamos, NM 87545

PVT relations in liquid and solid T_2 near the melting curve were measured over 20.5 K–22.1 K and 0 MPa–7 MPa (0 bar–70 bar) with a cell that used diaphragms for pressure and volume variation and measuremcnt. Because of ortho-para self conversion, the melting pressure P_m and the liquid molar volume V_{lm} increased with time. The rates wcre consistent with a second order rcaction similar to that for c the J = odd concentration:

$$dc/dt = -k_1c^2 + k_2c(1-c),$$

where $k_1 = 6 - 9 \times 10^{-2} h^{-1}$. By extrapolation, the ortho and para forms differed by $\Delta P_m \sim 6$ bar and $\Delta V_{lm} \sim 0.5\%$. Measurements of the volume change on melting and the thermal expansion and compressibility for liquid T_2 were consistent with those for H_2 and D_2. Impurities such as H_2, HT, DT, and ^{3}He were removed by a technique using an adsorption column of cold activated alumina. Corrections for ^{3}He growth during an cxpcriment were adequate except near the triple point.

Key words: deuterium; hydrogen; *PVT* relations; tritium.

Accepted: September 24, 1993

1. Introduction

Basic interest in the hydrogens H_2, D_2, and T_2 is notably enhanced by the existence of significant zero-point energy, large relative mass differences, and different ortho-para characteristics. In addition, D_2 and T_2 in the condensed phases are prime candidates as fuels for controlled nuclear fusion.

Although the discoveries of D_2 in 1931 [1] and T_2 in 1934 [2] were close together in time, the pressure-volume-temperature (*PVT*) measurements on T_2 have lagged far behind those on D_2. Essentially they were the 1951 measurements of vapor pressure [3] and liquid density [4] up to 3 bar[1] and 29 K and the 1956 melting curve determination up to 3100 bar and 60 K [5]. Contributing to the sluggishness of research efforts have been the high cost of T_2 and the difficulties that arise from its radioactivity (2.8 Ci/cm^3 STP gas). Health and environment concerns require great care in containing T_2 and definite provisions for accidental release. The continual creation of ^{3}He from nuclear decay automatically adds a significant impurity. Self-heating demands proper equipment design and/or data corrections. The exchange of tritium with hydrogen in equipment causes physical breakdown of plastics and contamination of the tritium with hydrogen. These problems have affected the accuracy and completeness of the data reported here.

[1] The bar (= 10^5Pa) is used in this paper rather than the pascal in order to facilitate the comparison of the results of this work with the results of previous and similar work. It should bc notcd that the International Committee for Weights and Measures allows the use of the bar temporarily with the International System of Units.

2. Apparatus and Procedures

The apparatus and procedures were basically those used for similar studies on ^{3}He [6], ^{4}He [7], D_2 [8], and H_2 [9]. The experimental cell consisted of three BeCu diaphragms welded at their circumferences and separated by 0.3 mm gaps. The lower gap, connected to a room-temperature He gas handling system via a capillary tube, had its pressure adjusted and measured directly. The upper gap was the T_2 experimental chamber and was connected to the room-temperature T_2 handling system via a low-temperature valve and a capillary tube. The sample pressure was determined from the deflection of the upper diaphragm, measured by electric capacitance. The experimental volume was determined from the pressures in the two gaps, using the calibrations described in Ref. [8].

The T_2 system is shown schematically in Fig. 1. Four stainless steel tanks, each of 1500 cm^3 volume, were used to hold T_2, either for storage or for transfer to various parts of the system. The T_2 was pumped at low pressure with a rotary vane pump and compressed to 70 bar with a diaphragm compressor. The uranium bed (U), Pd diffuser (Pd), and Al_2O_3 adsorption tube (Al_2O_3) were used for T_2 purification. T_2 gas samples were collected in sample tubes and analyzed by mass spectrometer. Calibration of capacitance versus cell pressure was done with the cell valve (V20) open and the T_2 separated from the oil piston gauge by a differential pressure indicator (DPI). To prevent excessive pressure in the cell upon loss of cooling when V20 was closed, a thermocouple on the cell signaled a motor to open V20, which allowed venting to a tank via a pressure relief valve (PRV). The plastic material in the cell valve tip and in the stem seals of the manipulative valves was the polyimide Vespel SP 211, which resisted the destructive action of T_2 quite well.

3. Purification

A significant problem in T_2 experiments is the growth of ^{3}He from radioactive decay at the rate of 0.031% per day. It was anticipated that a ^{3}He-T_2 mixture would behave like a ^{4}He-H_2 mixture in solubility and effect on *PVT* measurements. The ^{3}He growth during an experiment (at most 76 h long) was not expected to exceed solubility limits. Thus it was felt that the *PVT* measurements could be adequately corrected for ^{3}He growth during an experiment but it was mandatory that the experiment start with ^{3}He-free T_2. Several methods of removing ^{3}He were used. Exposure to U at 300 K binds T_2 as UT_3 and allows the unabsorbed ^{3}He to be pumped away but good removal requires several cycles. A Pd tube diffuser retains all gases except the hydrogens. But these methods are slow and do not remove hydrogen and deuterium, which are initially present or appear in the gas when most materials are exposed to T_2. Therefore the final process used was desorption from Al_2O_3, following basically the method of Depatie and Mills [10] for preparation of 99% o-H_2 or p-D_2. About 32 cm^3 of 2 mm dia. pellets of Al_2O_3 was placed in a 21 cm long stainless steel tube (15.3 mm O.D. and 0.28 mm wall). At the center of this was a stainless steel tube (3.2 mm O.D. and 0.25 mm wall) for with-

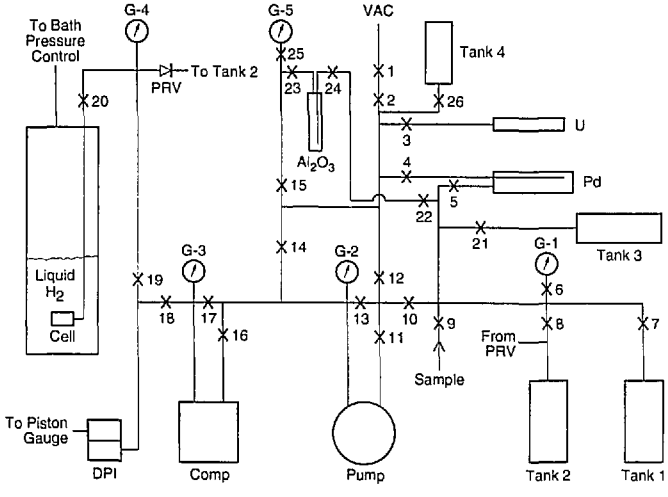

Fig. 1. Schematic of tritium *PVT* system.

drawing the gas. Prior to use, the Al_2O_3 was evacuated at 140 °C for 2 h. The impure gas was added to the Al_2O_3 tube immersed in liquid H_2 until saturation occurred at 87 mbar, after which it was passed through the tube at 87 mbar. The gas entered the top of the Al_2O_3 column and exited from the bottom until the exiting gas composition was the same as that of the entering gas, at which time flow was stopped. Then the liquid H_2 bath was lowered slowly until the effluent gas was almost pure T_2, after which the gas was collected separately while the adsorption tube warmed to room temperature. A pre-T_2 test on D_2 containing 0.61% HD produced 3500 cm^3 STP D_2 with 0.03% HD. For T_2 initially containing 0.26% H_2, 1.97% ^3He, 7.34% HT, and 0.49% DT, Table 1 gives the composition of effluent gas samples taken at various points of withdrawal. Collection of the gas after $V=1600$ cm^3 yielded 1600 cm^3 T_2 containing 0.18% H, 0.10% D, and < 0.01% ^3He which was enough for a *PVT* run.

Table 1. Gas composition (%) as a function of effluent volume

$V(cm^3STP)$	600	900	1200	1600	3200
H_2	3.71	0.080	0.064	0.046	0.028
^3He	0.90	0.010	<0.01	<0.01	<0.01
HT	75.84	5.66	0.36	0.38	0.20
DT	2.50	0.54	0.46	0.36	0.06
T_2	17.05	93.62	99.12	99.21	99.72

4. Ortho-Para Considerations

The equilibrium ortho-para composition in T_2 for various temperatures was calculated by Jones [11] and Gaines, Tsugawa, and Souers [12] and measured by Frauenfelder, Heinrich, and Olin [13]. The Gaines et al. results ($T \leq 22.5$ K) agreed fairly well with the Jones results, which covered 0 K–175 K. The measurements [13] gave somewhat higher values of c, the $J=$ odd concentration, which could result from a higher sample temperature than the thermometer reading because of the radioactive heating. The Jones calculation is used as the standard in this paper.

The equilibrium values c(e) versus temperature T for H_2, D_2, and T_2 are shown to 100 K in Fig. 2. The normal (n) values (those at $T=300$ K) are 0.75 for H_2 and T_2 and 0.33 for D_2. While c(e) for H_2 and D_2 at 20 K is very small and insensitive to T, c(e) = 0.34 for T_2 and increases rapidly with increasing T. Furthermore, the o-p conversion in T_2 is much faster than in H_2 under similar conditions. Therefore, it is important to determine c during the *PVT* measurements on T_2. The variations of c with time t and vapor pressure were measured and partially reported earlier [14]. There, the values of c were derived from gas thermal conductivity measurements on samples from the condensed phase, thus the rapid back conversion, p→o, in the gas phase decreased reliability somewhat. The best fits of the data were: for the solid,

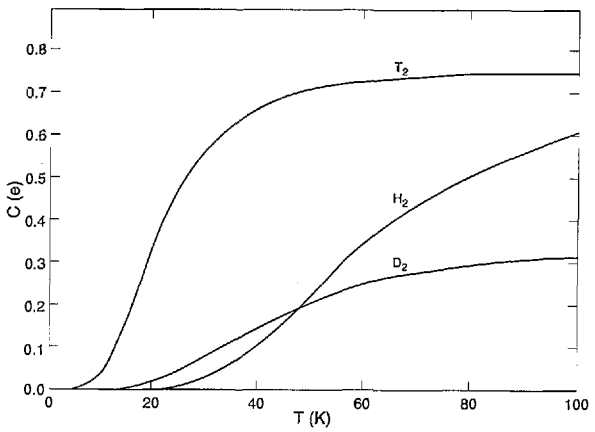

Fig. 2. Concentration of $J=$ odd states in the hydrogens at equilibrium vs temperature.

$$dc/dt = -kc^2 \quad (1)$$

and for the liquid,

$$dc/dt = -k_1c^2 + k_2c(1-c) \quad (2)$$

where k and k_1 are empirical rate constants and $k_2 = k_1c(e)/(1-c(e))$.

The results on o-p conversion are summarized in Table 2 in several useful forms: (a) r_0, the conversion rate at zero time; (b) $t_{1/2}$, the time to convert 1/2 way to equilibrium; and (c) k,k_1, and k_2, the rate constants. In solid T_2, the observed $t_{1/2}$ values of 2.0 h, 2.6 h, and 8.1 h at 4.0 K, 15.0 K, and 19.5 K, respectively, are moderately consistent with the NMR results of Gaines et al. [12] and Sater et al. [15] (although the latter found a minimum at 11.4 K) and with 1.5 h at 4 K of Frauenfelder et al. [13] using gas thermal conductivity analysis. However, Albers, Harteck, and Reeves [16] measured 0.28 h at 4 K with gas thermal conductivity. Our observed $t_{1/2}=8.3$ h in liquid at 20.7 K also agrees with the Gaines et al. result. Thus, the conversion rates are about the same in liquid and solid near the triple point (20.6 K), which simplifies interpreting the

Table 2. Ortho→para conversion in T_2 at vapor pressure

	Solid		
T(K)	4.0	15.0	19.5
c(e)	0	0.166	0.325
k(h^{-1})	0.675	0.321	0.065
r_0(%h^{-1})	38	18	4
$t_{1/2}$(h)	2.0	2.6	8.1
	Liquid		
T(K)	20.7		24.4
c(e)	0.358		0.460
k_1($10^{-2}h^{-1}$)	8.46		6.32
k_2($10^{-2}h^{-1}$)	4.72		5.40
r_0(%h^{-1})	3.9		2.5
$t_{1/2}$(h)	8.3		8.8

PVT measurements on a liquid/solid mixture. The value of $k_1 \sim 8\times10^{-2}h^{-1}$ is eight times the k_1 for H_2 given by Woolley, Scott, and Brickwedde [17].

Vapor pressures of T_2 at a certain c value, $P(c)$, and of n-T_2 P(n), were measured simultaneously in a special two-cell system. The differences, $\Delta P = P(c) - P(\text{n})$, are summarized in Table 3. Their behavior follows that of H_2 at similar values of P(n), as in Woolley et al. [17]. For example, extrapolation of the P(n) = 840 mbar data to $c = 0$ gives $\Delta P = 29$ mbar for T_2 and $\Delta P = 31$ mbar for H_2.

Table 3. Vapor pressure of T_2 at various ortho values

Phase	P(n) mbar	T K	c	ΔP mbar	$\Delta P/\Delta c$ mbar
liquid	840	24.4	0.66	6.0	67
liquid	840	24.4	0.54	12	57
liquid	840	24.4	0	(29)	(39)
liquid	228	20.7	0.48	4	15
solid	123	10.5	0.33	5.9	14
solid	116	19.4	0.46	4	14

In the *PVT* measurements above vapor pressure, gas thermal conductivity could not be used to determine c. Instead, the variations of melting pressure and liquid molar volume with time were used to determine o-p conversion rates. In these measurements, it was assumed that the initial value of c was 0.75 because: (1) the purification process left the T_2 sample at $c \sim 0.75$; and (2) the typical 2 h–5 h storage times at 300 K and 1.1 bar in a 1500 cm^3 SS tank before condensation promoted conversion to n-T_2.

5. Results

The *PVT* measurements typically began 2 h–3 h after condensation and continued for 50 h–76 h. Usually a single loading of the cell at a given T was used to measure compressibility and thermal expansion of liquid and solid, melting pressure, and volume change on melting. The liquid was compressed by a diaphragm until freezing began, which required 2 bar–4 bar overpressure. After the cell pressure stabilized, the compression was slowly continued past completion of freezing, which was indicated by a rapid rise in pressure.

5.1 Melting Pressures

The melting pressures P_m discussed here were the first-freeze values, obtained by extrapolation to zero amount of solid. If the compression was delayed, the increase in P_m with time was attributed to o-p conversion and ^{3}He growth. The o-p change seemed to follow Eq. (2) where $c = 0.75 - \Delta P_m/q$, $\Delta P_m = P_m(c) - P_m(c = 0.75)$, $q = \Delta P_m/(0.75 - c)$, and k_1 and q are constant at constant T. Measurements of P_m for ^{4}He-H_2 mixtures made up in the gas phase showed the regular effects of a slightly soluble gas and agreed fairly well with results of Bereznyak and Sheinina [18]. The mixture P_m increased 3 bar–4 bar per 1% of ^{4}He over the P_m range of 0 bar–70 bar. Since ^{3}He formation in T_2 is 1.29×10^{-3}% per hour, it was expected that ^{3}He dissolved in condensed T_2 would increase P_m by 3.7 mbar–5.0 mbar h^{-1}, which would necessitate small corrections. If saturation were exceeded, the ^{3}He would probably act as an ideal gas, i.e., V varies as P^{-1}. Thus, the correction would be 60 mbar h^{-1} at the lowest P_m (2.4 bar at 20.55 K), and 3.4 mbar h^{-1} at the highest P_m (70 bar). The ^{3}He growth in 76 h (the longest time after purification) is 0.098% whereas the ^{4}He-H_2 measurements in this cell and in Ref. [18] gave 0.16% ^{4}He as the solubility limit at 2.4 bar and 14 K. It follows that ^{3}He would be expected to stay in solution. However, it apparently had left solution at 20.55 K when P_m and liquid compressibility β_l were measured. Here the measured "P_m" was 2.4 bar, whereas linear extrapolation from higher T gave $P_m = 0$. If the excess pressure all came from ideal gas ^{3}He the solubility would be 0.046% ^{3}He. Sherman (R. H. Sherman, personal communication) measured 0.077%, which would result in 0.098–0.077 = 0.021% ^{3}He as gas at 0.97 bar, which would yield 1.4 bar as the real P_m. For this sample, the measured β_l was 10 times "normal," i.e., values

for T_2 aged 2 h–4 h. Furthermore, T_2 with 52 h–70 h ^{3}He growth at 20.60 K and 20.65 K showed β_1 to be 4–7 times "normal." These high β_1 values must have been the result of gas in the cell. The ^{4}He-H_2 mixtures containing up to 1% ^{4}He, but below saturation, never gave β_1 values greater than 10% above pure H_2 values. This throws suspicion on the high P_m and β_1 results for T_2.

Taylor [19] summarized some experiments on condensed T_2 in which ^{3}He had grown beyond the normal solubility limit. In liquid and solid T_2 there was a lack of vapor pressure buildup consistent with the ^{3}He production rate. In another case, analysis of successive aliquots of gas removed from aged liquid T_2 showed the last liquid was ^{3}He-rich. Supplementary evidence for ^{3}He not appearing as gas was provided by electrical conductivity and magnetic susceptibility measurements. The formation of free ^{3}He was visually observed by Hoffer (J. K. Hoffer, personal communication), who condensed DT near the triple point in a cylindrical cell with sapphire windows at the ends [20]. After 8 d as a liquid, the DT showed no bubbles. (They could not be hidden in the fill tube, for it entered the bottom of the cell.) After a freeze and a melt, the sample showed a bubble at the top of the cell with a volume that was ~1% of the ideal gas volume for 8 d ^{3}He growth. A second freeze and melt produced the same bubble, which persisted for 3 d. Then, within 12 h the bubble grew to 100% of the calculated volume for 12 d ^{3}He growth, taking up 20% of the cell volume. During the next three days no change in the bubble was seen, even after a freeze and a melt. The behavior of ^{3}He grown in condensed T_2 seems to be unpredictable.

For this paper, the P_m measurements were corrected as if the ^{3}He$-T_2$ sample formed a solution like ^{4}He-H_2. Figure 3 shows $\Delta P_m = P_m(t) - P_m(0)$ at 20.650 K, 21.900 K, and 22.100 K with and without ^{3}He corrections. If the high rate at 20.65 K was caused by ^{3}He growth, it seems that a greater correction is needed. In the fit to Eq. (2), q and the initial ΔP_m were varied to get the most consistent k_1 for each run. The results, summarized in Table 4, show the similarities with the time variation of c in liquid at vapor pressure (Table 2). The average value $q = 6.0$ agrees with the H_2 values 5.7–6.4 over 14 K–16 K from: P_m(p) by Youngblood [21]; P_m(n) by Mills and Grilly [5]; and P_m(p) and P_m(n) in the present apparatus.

Regardless of the previous discussion, extrapolation of P_m ($t < 6$ h) to $t = 0$ gave P_m(n). For e-T_2, values of P_m(e) with ^{3}He corrections were obtained from q values or $P_m(t \sim 50$ h). Corrections for

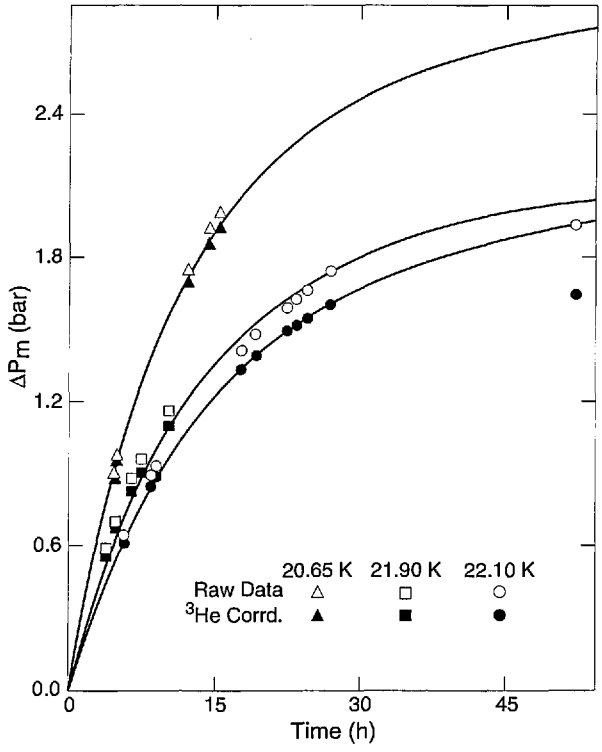

Fig. 3. Tritium melting pressure vs time at several temperatures.

Table 4. Ortho→para conversion in T_2 from melting pressure change. Results in parentheses are from data uncorrected for ^{3}He

T(K)	20.65	21.90	22.10
P_{m0}(bar)	3.295	58.630	67.906
c(e)	0.358	0.393	0.400
$k_1(10^{-2}h^{-1})$	7.90(8.00)	6.58(7.00)	5.46(5.58)
$k_2(10^{-2}h^{-1})$	4.41(4.46)	4.26(4.53)	3.64(3.70)
$r_0(\%h^{-1})$	3.62(3.66)	2.90(3.09)	2.39(2.44)
$t_{1/2}$(h)	8.86(8.74)	9.89(9.30)	11.76(11.54)
q(bar)	7.4(7.6)	6.1(6.2)	6.1(6.5)

0.08%–0.42% H content ($H_2\% + 1/2HT\%$) were made at the rate of -1.7 bar per 1% H. The results are summarized in Table 5, illustrated in Fig. 4 for $P_m < 25$ bar, and, over 20.83 K–22.10 K, fit the equations:

$$P_m(n) = 0.22 + 45.92\ (T - 20.627)\ \text{bar}, \quad (3)$$

$$P_m(e) = 0.22 + 45.27\ (T - 20.568)\ \text{bar}. \quad (4)$$

The constant 0.22 is the triple point pressure for n-T_2 determined from vapor pressure measurements [3], and it is assumed for e-T_2 as well. The linear $P_m - T$ relation corresponds with the H_2 and D_2 curves. The greater values just above the triple

Table 5. Melting pressure of T_2

T K	H%[a]	P(n) bar	$P-P_{eq}$ bar	c(e)	t[b] h	P(e)[c] bar	$P-P_{eq}$ bar	q bar
20.550	0.13			0.356	71	2.145[d]		
20.650	0.13	3.295[d]	+2.02	0.358		(6.196[d])	+2.26	7.4
20.700	0.21	4.722[d]	+1.15	0.359	52	7.053[d]	+0.86	6.0
20.900	0.08			0.365	42	15.235	−0.01	6.4
21.000	0.08	17.419	+0.07	0.368		(19.864)	+0.09	6.4
21.000	0.21			0.368	68	19.772	0.00	6.2
21.050	0.22	19.632	−0.01	0.370		(22.140)	+0.10	6.6
21.100	0.42	21.968	+0.03	0.371	53	24.469	+0.16	6.6
21.390	0.15	35.198	−0.06	0.379		(37.239)	−0.19	5.5
21.600	0.35	44.660	−0.24	0.385				5.6
21.700	0.10			0.388	56	51.593	+0.12	5.8
21.750	0.25	51.751	−0.04	0.389	58	53.377	−0.35	4.5
21.900	0.10	58.630	−0.05	0.393				6.1
22.100	0.15	67.906	+0.05	0.400		(70.041)	+0.48	6.1
22.100	0.15			0.400	52	69.574	0.00	4.8

[a] Corrections to P were made at the rate of −1.7 bar for 1% H.
[b] t was the time in the condensed state when P(e) was measured.
[c] Values in parentheses are from Eq. (2) fitting.
[d] See text for the uncertainty involved.

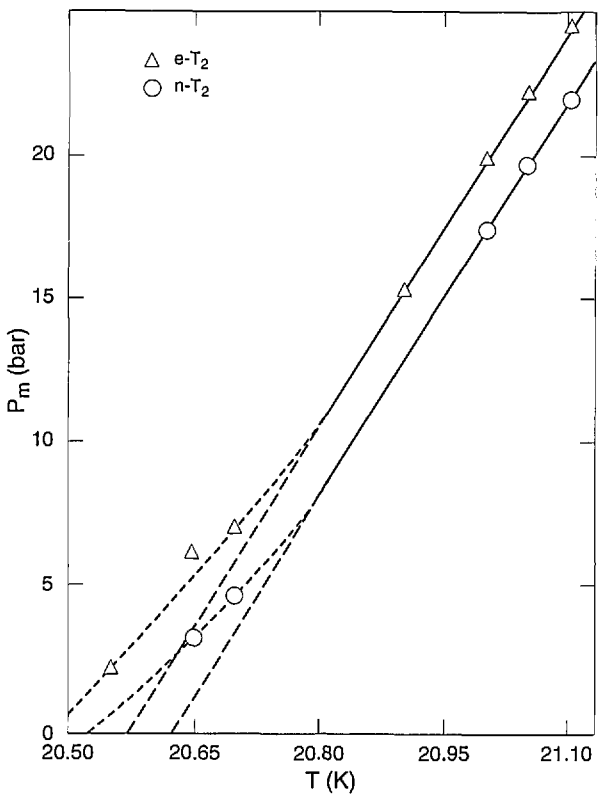

Fig. 4. Tritium melting pressure vs temperature.

point, as shown in Fig. 4, cannot be resolved at present. If Eqs. (3) and (4) held down to the triple point, the T_{tp} values would be 20.627 K for n-T_2 and 20.568 K for e-T_2. The 20.627 K value is close to T_{tp}(n-T_2) = 20.62 K, the junction of the liquid and solid vapor pressure equations [3]. Unfortunately, those equations ignored the highest point measured in the solid region, 2.116 bar at 20.547 K. If the liquid and solid curves went through that point, T_{tp}(n-T_2) would be 20.547 K, falling between the possible values from the melting curve, 20.53 K and 20.62 K. The T_{tp}(e-T_2) seems to be in the 20.48 K–20.57 K range. In Table 5, $P-P_{eq}$ is the difference between experimental and equation values of P_m.

The sole previous P_m measurement in the present range was 56.68 bar at 21.826 K for n-T_2 by Mills and Grilly [5], which is 1.48 bar higher than the present result. Of this deviation, 0.76 bar could be from the 0.9% HT impurity in the earlier measurement. Their equation gives values that are lower than the present by 2.5 bar. An equation devised by Goodwin [22] gives values lower than the present by 0.64 bar.

5.2 Volume Change with Time

The increase with time seen in liquid volume V_l at constant T and $P(\sim P_m)$ was also attributed to o-p conversion and ^{3}He growth. The data fit Eq.(2) where $c = 0.75 - \Delta V_l/sV_l$, $\Delta V_l = V_l(c) - V_l(c = 0.75)$, and $s = \Delta V_l/(0.75 - c)V_l$ with $k_l = 7.53 \times 10^{-2}\text{h}^{-1}$ and $s = 5.7 \times 10^{-3}$ for the raw values of $\Delta V_l/V_l$ at 21.00 K (c(e) = 0.368) and 14.86 bar. In Fig. 5, the raw data deviate from the dashed equation curve, indicating

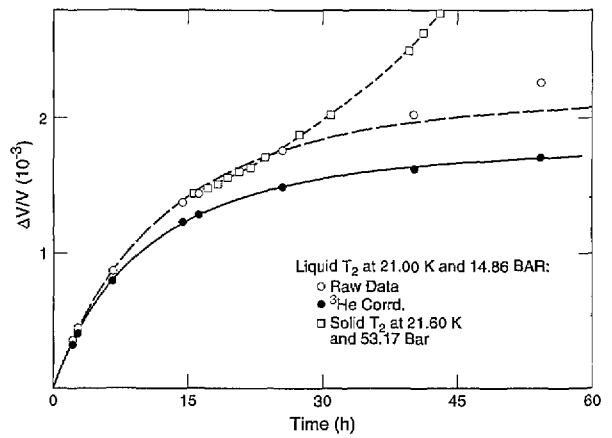

Fig. 5. Relative volume change of T_2 vs time.

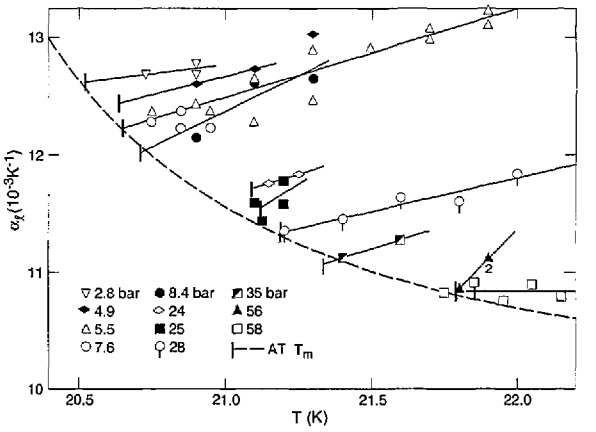

Fig. 6. Thermal expansion of liquid e-T_2 vs temperature at various pressures.

that o-p conversion almost stops after 30 h and thereafter V_l increases mostly from ^{3}He growth. An empirical correction to $\Delta V_l/V_l$, $-1.0\times10^{-5}h^{-1}$, to yield coincidence between the corrected data and the solid equation curve results in $k_l = 8.98\times10^{-2}h^{-1}$ and $s = 4.6\times10^{-3}$. The k_l values are similar to the results from P_m (Table 4), but the s values are smaller than the values for H_2: 6.5×10^{-3} by Scott and Brickwedde [23] at vapor pressure; 6.7×10^{-3} by Wallace and Meyer [24] at P_m. Measurements of $\Delta V/V$ vs t on solid T_2 at 21.600 K and 53.17 bar were begun after the sample had been liquid for 6 h and solid for 9.5 h. They were added to the 21.000 K liquid value at $t = 15.5$ h. The results, shown in Fig. 5, follow the liquid curve for 9 h before rising sharply, probably because of breakup of the solid.

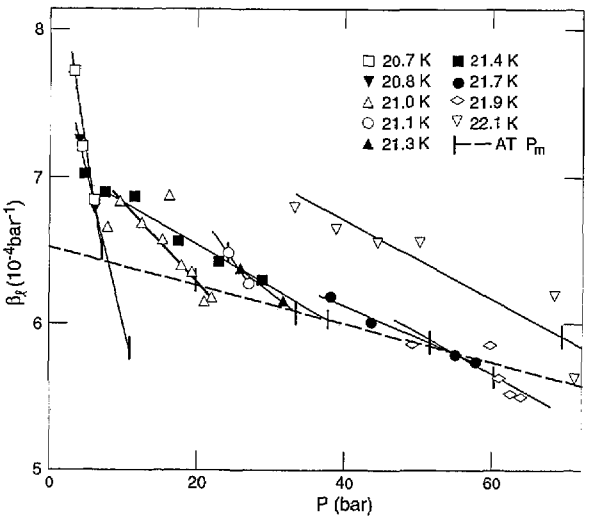

Fig. 7. Compressibility of liquid e-T_2 vs pressure at various temperatures.

5.3 Liquid Thermal Expansion and Compressibility

The thermal expansion coefficient, $\alpha = V^{-1}(\partial V/\partial T)_P$, and the compressibility coefficient, $\beta = -V^{-1}(\partial V/\partial P)_T$, of the liquid were measured directly. All α and 2/3 of the β measurements were made on essentially e-T_2. The measurements at $c = 0.6$–0.7 fit in with the others. They would require a $+1.5\%$ correction, at most, for the volume change from o-p conversion during the 5 min measurement, and this is within the scatter of data. The differences in α and β for n-H_2 and e-H_2 were found to be within 2%. Therefore, it is assumed that the T_2 data are independent of c. The α results are given in Fig. 6 as functions of T at various pressures. The dashed curve is through T_m of e-T_2. The β results are shown in Fig. 7 as functions of P at various temperatures, and the dashed curve is through P_m of e-T_2.

There are no other data on α or β for T_2. Comparison of α for H_2, D_2 [8] and T_2 is shown in Fig. 8. The three isotopes show similar slopes $(\partial\alpha/\partial T)_P$ and their α values come together with pressure, becoming equal at 57 bar. Figure 9 shows β for the isotopes tending to merge at high pressures.

5.4 Molar Volumes

The molar volume of liquid T_2 along the melting curve V_{lm} was calculated from the measurement at the triple point [4], 22.051 cm^3mol^{-1} for n-T_2, and the measured α and β values. This V_{lm} multiplied by the measured $\Delta V_m/V_{lm}$ yielded ΔV_m, the volume change on melting. Finally, the solid molar volume

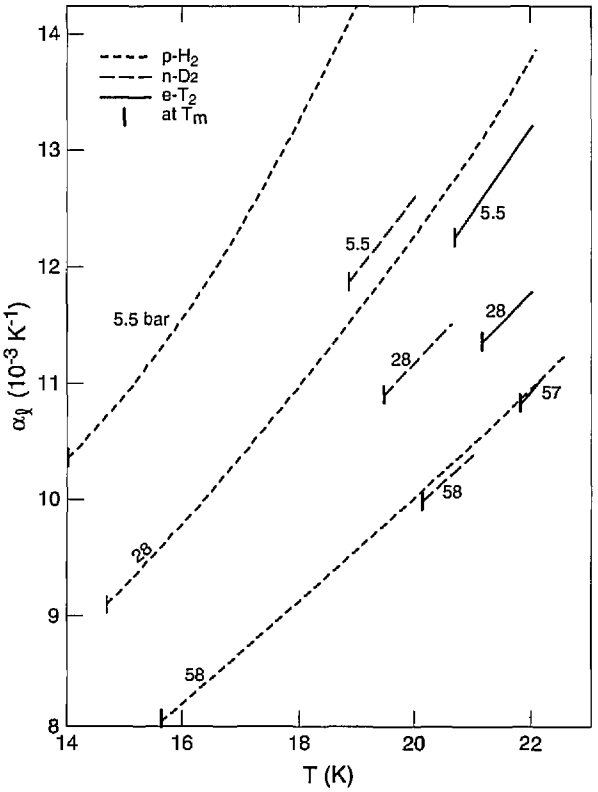

Fig. 8. Liquid thermal expansion of the hydrogens vs temperature at several pressures.

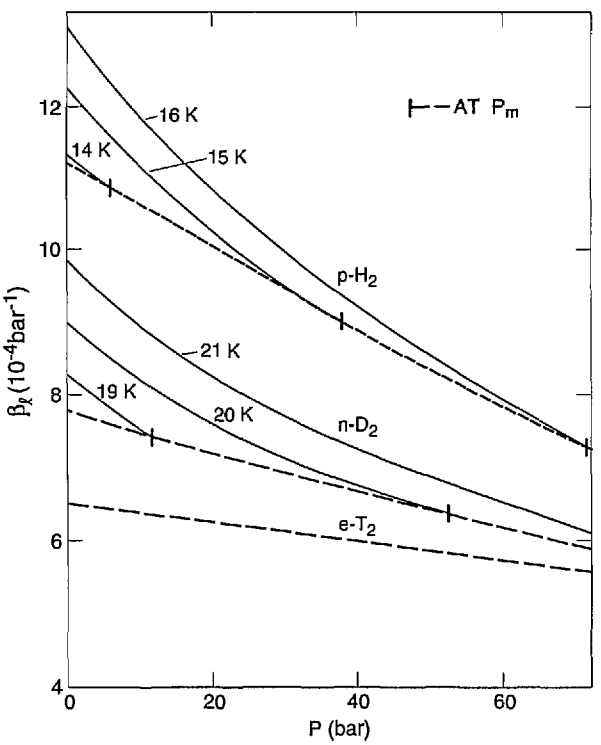

Fig. 9. Liquid compressibility of the hydrogens vs pressure at several temperatures.

V_{sm} was determined from $V_{lm} - \Delta V_m$. Figures 10 and 11 give the results on $\Delta V_m/V_{lm}$ and ΔV_m, respectively, for T_2, H_2, and D_2 [8]. Essentially, the $\Delta V_m/V_{lm}$ curves show a parallel displacement for the isotopes while the ΔV_m curves are fairly close together. The results are given in Table 6. All the smoothed *PVT* values along the melting curve are summarized in Table 7 which should be self-consistent. Here, the V_{lm} and V_{sm} values are for n-T_2, but the values for e-T_2 are only slightly larger. Values of V_{lm}(e-T_2) − V_{lm}(n-T_2) were calculated from the o-p expansion and the P_m (n-T_2)→P_m (e-T_2) contraction, using the s values in Table 4 and the β values in Table 7. The two effects largely cancel

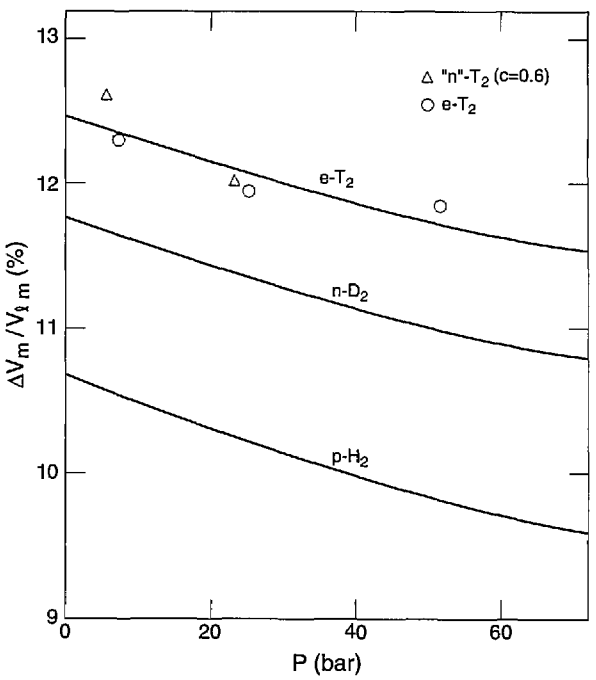

Fig. 10. Relative volume change on melting of the hydrogens.

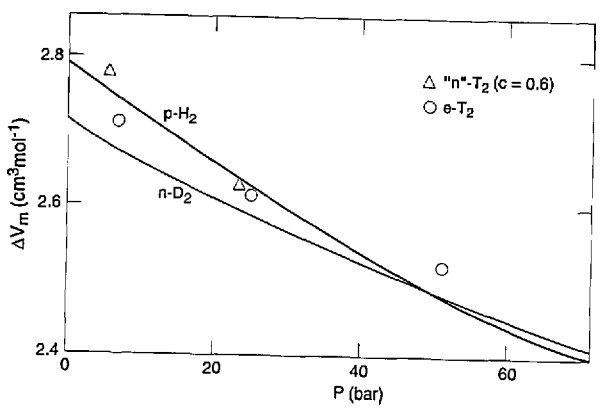

Fig. 11. Volume change on melting of the hydrogens.

Table 6. Volume change on melting of T_2

T K	P_m[a] bar	$\Delta V_m/V_{lm}$[a] %	V_{lm} cm^3mol^{-1}	ΔV_m cm^3mol^{-1}	V_{sm} cm^3mol^{-1}
			n-T_2		
20.700	4.72	12.62	22.024	2.779	19.245
21.100	22.23	12.02	21.881	2.630	19.251
			e-T_2		
20.700	7.05	12.30	22.026	2.709	19.317
21.100	24.47	11.95	21.883	2.615	19.268
21.700	51.59	11.86	21.659	2.569	19.090

[a] Direct measurement.

Table 7. Properties of T_2 along the melting curve

T K	P(n-T_2) bar	P(e-T_2) bar	c(e)	α_l 10^{-3} K^{-1}	β_l 10^{-4} bar^{-1}	V_l(n-T_2) cm^3mol^{-1}	V_l(e-T_2) cm^3mol^{-1}	$\Delta V_m/V_l$ %	ΔV_m cm^3mol^{-1}	V_s(n-T_2)[b] cm^3mol^{-1}
20.535[a]	0.22	1.80	0.357	12.4	6.85	22.051	22.060	12.40	2.734	19.317
20.700	4.72	7.05	0.359	12.2	6.79	22.024	22.026	12.35	2.720	19.304
20.800	8.30	10.80	0.362	12.0	6.72	21.995	21.997	12.29	2.703	19.292
20.900	12.76	15.24	0.365	11.9	6.65	21.959	21.961	12.22	2.683	19.276
21.000	17.35	19.77	0.368	11.7	6.59	21.920	21.922	12.15	2.663	19.257
21.100	21.94	24.30	0.371	11.6	6.51	21.881	21.883	12.08	2.643	19.238
21.200	26.53	28.87	0.374	11.4	6.45	21.842	21.844	12.01	2.623	19.219
21.300	31.12	33.36	0.377	11.2	6.39	21.804	21.806	11.95	2.606	19.198
21.400	35.72	37.88	0.379	11.1	6.32	21.766	21.768	11.89	2.588	19.178
21.500	40.31	42.41	0.382	11.0	6.24	21.728	21.730	11.83	2.570	19.158
21.600	44.90	46.94	0.385	10.9	6.16	21.691	21.694	11.77	2.553	19.138
21.700	49.49	51.47	0.388	10.9	6.10	21.655	21.659	11.72	2.538	19.117
21.800	54.08	56.00	0.390	10.8	6.04	21.618	21.624	11.67	2.523	19.095
21.900	58.68	60.52	0.393	10.8	5.97	21.582	21.589	11.62	2.508	19.074
22.000	63.27	65.05	0.396	10.7	5.90	21.547	21.555	11.58	2.495	19.052
22.100	67.86	69.57	0.400	10.7	5.82	21.512	21.521	11.54	2.482	19.030

[a] See text on the triple point.
[b] V_s(e-T_2) − V_s(n-T_2) = V_l(e-T_2) − V_l(n-T_2).

each other, leaving a net difference of only 0.002 cm^3mol^{-1} for the most part, with high values of 0.009 at 20.535 K and 22.1 K. The result is carried over to V_{sm} since $\Delta V_m/V_{lm}$ is assumed to be independent of c.

The possibility of comparison with other work is small. Hammel [25] predicted $\Delta V_m = 2.66$ cm^3mol^{-1} at the triple point, whereas here we get 2.734. Driessen et al. [26] calculated values of V_{sm} that are 0.05 cm^3mol^{-1}–0.07 cm^3mol^{-1} lower than ours over 20.535 K–22.1 K range.

5.5 Solid Thermal Expansion and Compressibility

The measurements of α and β for the solid phase gave erratic and probably low values in general. This behavior can be expected from poor pliability of the solid in the measuring cell, which tends to be worse away from the melting curve [8]. The behavior occurred in all the isotopes, but T_2 has other properties that could influence the measurements: ^3He production, internal heating, and solid fracturing. Although the measurements were made on e-T_2 the results can probably be used for any o-p composition.

For each of H_2, D_2, and T_2, α was measured at several pressures as a function of T, and each time it increased with T. However, α at constant T generally decreases with P. Thus the extrapolations of α to T_m can lead to roughly constant values, which occurs for H_2 and D_2 [8]. However α increases with T_m for T_2. Figure 12 illustrates these behaviors,

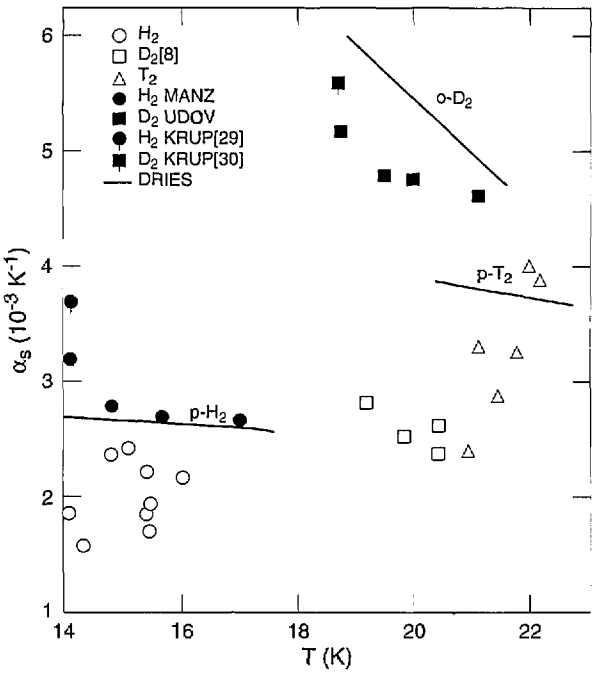

Fig. 12. Solid thermal expansion of the hydrogens along the melting curve. MANZ is Manzhelii et al. [27]; UDOV is Udovidchenko et al. [28]; KRUP [29] is Krupskii et al. [29]; KRUP [30] is Krupskii et al. [30]; DRIES is Driessen et al. [26].

along with the overall increase in α from H_2 to D_2 to T_2. The results of Driessen et al. [26] are also shown there. They measured the isochores of p-H_2 and o-D_2 up to 2 kbar, between the melting curve and 4.2 K, by use of a cell whose wall deflections were measured with strain gauges. Molar volumes were determined by correlation with data at the melting line and 4.2 K. Isochores were fit by integration of specific heat. The resulting equation of state was used to calculate V, α, and β up to 25 kbar. The derivation of an EOS for p-T_2 was "guided by experimental results for H_2 and D_2." Their α results appear to be in rough agreement with ours for H_2 and T_2 but for D_2 they are about twice as great. Densities were derived from dielectric constant measurements on p-H_2 by Manzhelii et al. [27] and on n-D_2 by Udovidchenko et al. [28]. Their α results (good to $\pm 10\%$), shown in Fig. 12, match the Driessen et al. results for H_2 very well and for D_2 within 15%. From x-ray studies of lattice parameters, Krupskii et al. [29,30] derived α for p-H_2 that is 37% higher than the Driessen et al. result and α for o-D_2 that is 8% lower.

The measurements of β as a function of P at several temperatures show a decrease with P. Generally, β increases with T, therefore, the extrapolated values of β to P_m can be almost constant, as illustrated in Fig. 13. There is also a big decrease in β from H_2 to D_2 to T_2. The values for H_2, D_2 [8], and T_2 are about 0.90, 0.55, and 0.77, respectively, of the Driessen et al. [26] results. The measurements of Manzhelii et al. [27] and of Udovidchenko and Manzhelii [31] on β of p-H_2 are 5%–10% greater than those of Driessen et al. [26] while the values of Udovidchenko et al. [28] for n-D_2 are slightly lower. Other measurements on H_2 and D_2 were made at 4.2 K using various direct and indirect techniques. In general, the values are low. In some cases, values of P were not low enough to allow satisfactory extrapolations.

In spite of these discrepancies in α and β results, there is hope for more accurate values for T_2. Overall, the Driessen et al. [26] results on H_2 and D_2 fit in fairly well with others. It follows that their T_2 results should be credible. For example, the change in V_s along the melting curve between 20.5

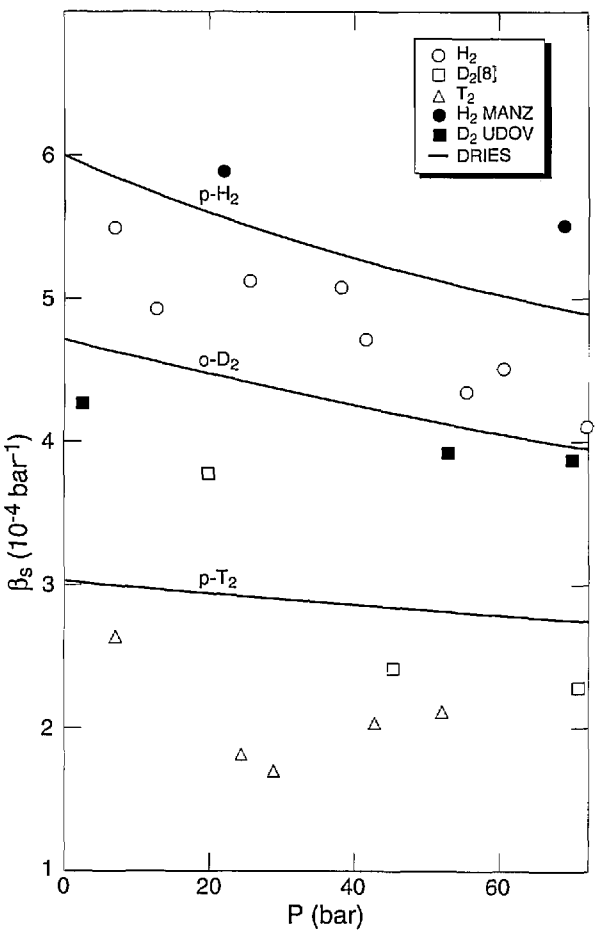

Fig. 13. Solid compressibility of the hydrogens along the melting curve. MANZ is Manzhelii et al. [27,31]; UDOV is Udovidchenko et al. [28]; DRIES is Driessen et al. [26].

K and 22.1 K is calculated from their α and β values to be 0.252 cm^3mol^{-1}, in reasonable agreement with $\Delta V_s = 0.287$ in Table 7.

In solid H_2 and D_2, some anomalies in α and β were observed [8] but hardly deserve recognition as phase change effects. There is no point adding to the confusion in this subject [27, 28, 29, 30, 32, 33]. In T_2, no anomaly was recognized, but observation was very limited.

5.6 Thermal Results

The enthalpy change on melting (heat of fusion) calculated from the Clapeyron equation $\Delta H_m = T\Delta V_m dP_m/dT$, using the present PVT measurements on n-T_2, is almost constant at 255 $Jmol^{-1}$ in the range 20.9 K–22.1 K or 13 bar–70 bar. However, below 20.9 K the rapid decrease in dP_m/dT lowers it to 144 $Jmol^{-1}$ at T_{tp}. On the other hand, ΔH_m for H_2 and D_2 varies linearly with P_m over 0 bar–70 bar from 117 $Jmol^{-1}$ to 130 $Jmol^{-1}$ for p-H_2, according to Dwyer et al. [34], and from 197 to 210 for n-D_2 [8]. If we wish to focus more on the similarities of the isotopes, perhaps it would be better to compare the behavior of the entropy change $\Delta S_m = \Delta H_m/T$. This decreases over 13 bar–70 bar by 2% for H_2 and D_2 and by 4% for T_2.

6. Summary

The PVT relations in liquid and solid T_2 were measured near the melting curve over 20.5 K–22.1 K and 0 bar-70 bar. They were compared with measurements on H_2 and D_2 and with calculations on T_2. Comparison of the three isotopes leads to few surprises. The melting pressure variations with temperature and ortho-para composition are consistent. An exception is the strange behavior of P_m for T_2 in the 0.3 K interval just above the triple point. The o-p conversion in condensed T_2 is faster than in H_2 but slow enough to allow observation of its effect on the PVT relations. The liquid and solid molar volumes of the three isotopes are consistent in magnitude and in their variations with o-p composition, pressure, and temperature. Still unresolved is the status of ^3He produced in condensed T_2.

Acknowledgment

I thank J. K. Hoffer and R. H. Sherman for sharing their observations on ^3He in condensed T_2.

7. References

[1] H. C. Urey, F. G. Brickwedde, and G. M. Murphy, Phys. Rev. **39**, 164 (1932).
[2] M. L. E. Oliphant, P. Harteck, and Lord Rutherford, Proc. Roy. Soc. **144 A**, 692 (1934).
[3] E. R. Grilly, J. Am. Chem. Soc. **73**, 843 (1951).
[4] E. R. Grilly, J. Am. Chem. Soc. **73**, 5307 (1951).
[5] R. L. Mills and E. R. Grilly, Phys. Rev. **101**, 1246 (1956).
[6] E. R. Grilly, J. Low Temp. Phys. **4**, 615 (1971).
[7] E. R. Grilly, J. Low Temp. Phys. **11**, 33 (1973).
[8] L. A. Schwalbe and E. R. Grilly, J. Res. Natl. Bur. Stand. (U.S.) **89**, 227 (1984).
[9] L. A. Schwalbe and E. R. Grilly, J. Res. Natl. Bur. Stand. (U.S.) **89**, 317 (1984).
[10] D. A. Depatie and R. L. Mills, Rev. Sci. Instr. **39**, 105 (1968).
[11] W. M. Jones, J. Chem. Phys. **16**, 1077 (1948).
[12] J. R. Gaines, R. T. Tsugawa, and P. C. Souers, Phys. Rev. Lett. **42**, 1717 (1979).
[13] R. Frauenfelder, F. Heinrich, and J. B. Olin, Helv. Phys. Acta **38**, 279 (1965).
[14] E. R. Grilly, Proceedings of the Third International Conference on Low Temperature Physics and Chemistry, Houston (1953) p. 66.
[15] J. D. Sater, J. R. Gaines, E. M. Fearon, P. C. Souers, F. E. McMurphy, and E. R. Mapoles, Phys. Rev. B **37**, 1482 (1988).
[16] E. W. Albers, P. Harteck, and R. R. Reeves, J. Amer. Chem. Soc. **86**, 204 (1964).
[17] H. W. Woolley, R. B. Scott, and F. G. Brickwedde, J. Res. Natl. Bur. Stand. (U.S.) **41**, 454 (1948).
[18] N. G. Bereznyak and A. A. Sheinina, Fiz. Nizk. Temp. **7**, 685 (1981). [Sov. J. Low Temp. Phys. **7**, 335 (1981)].
[19] R. D. Taylor, Proceedings of the 17th International Conference on Low Temperature Physics, Karlsruhe, 1984, part II, Paper EL 10.
[20] J. K. Hoffer and L. R. Foreman, Phys. Rev. Lett. **60**, 1310 (1988).
[21] B. A. Youngblood, J. Chem. Phys. **48**, 4181 (1968).
[22] R. D. Goodwin, Cryogenics **2** (6) 353 (1962).
[23] R. B. Scott and F. G. Brickwedde, J. Res. Natl. Bur. Stand. (U.S.) **19**, 237 (1937); J. Chem. Phys. **5**, 736 (1937).
[24] B. A. Wallace and H. Meyer, Proceedings of the 13th International Conference on Low Temperature Physics, Boulder, CO, Vol. 2 (1972) p. 194.
[25] E. F. Hammel, J. Chem. Phys. **18**, 228 (1950).
[26] A. Driessen, Thesis, Univ. of Amsterdam (1982); A. Driessen and I. F. Silvera, J. Low Temp. Phys. **54**, 565 (1984).
[27] V. G. Manzhelii, B. G. Udovidchenko, and V. B. Esel'son, Fiz. Nizk Temp. **1**, 799 (1975). [Sov. J. Low Temp. Phys. **1**, 384 (1975)]. Also: V. G. Manzhelii, B. G. Udovidchenko, and V. B. Esel'son, Zh. Eksp. Teor. Pisma **18**, 30 (1973). [Sov. Phys.-JETP Letters **18**, 16 (1973)]. B. G. Udovidchenko, V. G. Manzhelii, and V. B. Esel'son, Phys. Status Solidi (a) **19**, K189 (1973).
[28] B. G. Udovidchenko, V. B. Esel'son, and V. G. Manzhelii, Fiz. Nizk Temp. **10**, 13 (1984). [Sov. J. Low Temp. Phys. **10**, 5 (1984)].
[29] I. N. Krupskii, A. I. Prokhvatilov, and G. N. Sheherbakov, Fiz. Nizk. Temp. **9**, 83 (1983). [Sov. J. Low Temp. Phys. **9**, 42 (1983).

[30] I. N. Krupskii, A. I. Prokhvatilov, and G. N. Shcherbakov, Fiz. Nizk Temp. **10**, 5 (1984). [Sov. J. Low Temp. Phys. **10**, 1 (1984)].
[31] B. G. Udovidchenko and V. G. Manzhelii, J. Low Temp. Phys. **3**, 429 (1970).
[32] N. G. Bereznyak and A. A. Sheinina, Fiz. Nizk Temp. **6**, 1255 (1980) [Sov. J. Low Temp. Phys. **6**, 608 (1980)].
[33] G. N. Shcherbakov, A. I. Prokhvatilov, and I. N. Krupskii, Fiz. Nizk Temp. **11**, 521 (1985). [Sov. J. Low Temp. Phys. **11**, 284 (1985)].

About the author: *E. R. Grilly is a physicist retired from the Condensed Matter and Thermal Physics Group of Los Alamos National Laboratory, in which this work was done.*